Wake pattern and wave resistance for anisotropic moving disturbances

Michael Benzaquen,[1] Alexandre Darmon,[2] and Elie Raphaël[1,a]

[1]*PCT, UMR CNRS 7083 Gulliver, ESPCI ParisTech PSL Research University, 10 rue Vauquelin, 75005 Paris, France*
[2]*EC2M, UMR CNRS 7083 Gulliver, ESPCI ParisTech PSL Research University, 10 rue Vauquelin, 75005 Paris, France*

We present a theoretical study of gravity waves generated by an anisotropic moving disturbance. We model the disturbance by an elliptical pressure field of given aspect ratio $\mathcal{W}$. We study the wake pattern as a function of $\mathcal{W}$ and the longitudinal hull Froude number $Fr = V/\sqrt{gL}$, where V is the velocity, g is the acceleration of gravity, and L is the size of the disturbance in the direction of motion. For large hull Froude numbers, we analytically show that the rescaled surface profiles for which $\sqrt{\mathcal{W}}/Fr$ is kept constant coincide. In particular, the angle outside which the surface is essentially flat remains constant and equal to the Kelvin angle, and the angle corresponding to the maximum amplitude of the waves scales as $\sqrt{\mathcal{W}}/Fr$, thus showing that previous work on the wake's angle for isotropic objects can be extended to anisotropic objects of given aspect ratio. We then focus on the wave resistance and discuss its properties in the case of an elliptical Gaussian pressure field. We derive an analytical expression for the wave resistance in the limit of very elongated objects and show that the position of the speed corresponding to the maximum wave resistance scales as $\sqrt{gL}/\sqrt{\mathcal{W}}$. © 2014 AIP Publishing LLC. [http://dx.doi.org/10.1063/1.4896257]

I. INTRODUCTION

The influence of Lord Kelvin's theory[1] on the study of water waves and particularly on the wake pattern that falls behind an object moving at constant speed is no longer to be proved. His work revealed a certain universality of the wake pattern, that everyone can notice when looking at the waves produced by objects as different as swans or sailing boats. One of his most remarkable results concerns the well-known constant wake angle $\varphi_K \simeq 19.47°$, delimiting a region outside which the water remains essentially unperturbed. Since Lord Kelvin's first results, a lot of efforts have been done to extend his work,[2–5] for instance to nonlinear waves,[6] or waves in the presence of vorticity.[7,8] Recently, the constancy of the wake angle has been contested.[9,10] Indeed, in their analysis of airborne images, *Rabaud and Moisy* showed that, for large hull Froude numbers $Fr = V/\sqrt{gL}$, where V is the object velocity, g is the acceleration of gravity, and L is the typical size of the object in the direction of motion, the angle of the wake decreases and scales as $1/Fr$. In response to these intriguing observations, we recently[11] presented an analytical study of the wake pattern as a function of the Froude number and showed that the delimiting angle of the wake actually remains constant for all Fr, therefore comforting Lord Kelvin's theory. We also provided an explanation to the airborne observations of *Rabaud and Moisy* by analytically proving that, for an axisymmetric object of typical size L, the angle corresponding to the maximum amplitude of the waves decreases as Fr is increased, scaling as $1/Fr$ for large Froude numbers.

The main issue that arose from our previous study[11] is that an axisymmetric object does not correctly reflect the real geometry of boats.[12] Indeed, boats have elongated shapes with aspect ratios

---

a)Electronic mail: elie.raphael@espci.fr

26, 092106-1

typically ranging between 0.1 and 0.5, with the exception of hovercrafts which actually display a cylindrical symmetry. For elongated objects, the emphasis has been placed on the planning regime in the limit of small aspect ratios.[13, 14] The important feature that needs to be considered when it comes to hull design, is the so-called wave resistance, or wave drag, a force resulting from the generation of surface waves. Indeed, a well profiled hull noticeably reduces the wave resistance thus improving the velocity performances of the ship. Along with wake patterns, wave resistance has been widely studied both at practical[15, 16] and theoretical levels.[2, 17, 18]

We here present a theoretical study on anisotropic moving objects. In the first part, we focus on the wake pattern. After recalling the main ingredients of the physical model, we calculate the surface displacement induced by an elliptical moving pressure distribution and discuss its main features. In particular, we investigate the universality of the wake pattern as a function of the aspect ratio of the moving disturbance and the longitudinal hull Froude number. In the second part, we derive the expression of the wave resistance for an anisotropic moving disturbance and focus on the case of an elliptical Gaussian pressure field. In the limit of very elongated objects, we obtain interesting analytical results on the scaling of the velocity corresponding to the maximum of the wave resistance.

II. WAKE PATTERN

For gravity waves, the surface displacement generated by a pressure field $p(x, y)$ moving in the $-x$ direction with constant speed V can be written in the frame of reference of the moving perturbation as[11, 17, 19]

$$\zeta(x, y) = -\lim_{\varepsilon \to 0} \iint \frac{\mathrm{d}k_x \, \mathrm{d}k_y}{4\pi^2 \rho} \frac{k \, \hat{p}(k_x, k_y) \, e^{-i(k_x x + k_y y)}}{\omega(k)^2 - V^2 k_x^2 + 2i\varepsilon V k_x} , \tag{1}$$

where $k = \left(k_x^2 + k_y^2\right)^{1/2}$, $\hat{p}(k_x, k_y)$ is the Fourier Transform of $p(x, y)$, ρ is the water density and $\omega(k) = (gk)^{1/2}$ is the dispersion relation for pure gravity waves. Let us nondimensionalise the problem through $x = LX$; $y = LY$; $k_x = K_X/L$; $k_y = K_Y/L$; $k = K/L$; $p = \rho g L \, P$; $\hat{p} = \rho g L^3 \hat{P}$; $\varepsilon = (g/L)^{1/2} \tilde{\varepsilon}$ where L is the typical size of the pressure field $p(x, y)$ in the direction of motion. This yields $\zeta(x, y) = (L/4\pi^2) Z(X, Y)$ where

$$Z(X, Y) = -\lim_{\tilde{\varepsilon} \to 0} \iint \mathrm{d}K_X \, \mathrm{d}K_Y \frac{K \hat{P}(K_X, K_Y) \, e^{-i(K_X X + K_Y Y)}}{K - Fr^2 K_X^2 + 2i\tilde{\varepsilon} \, Fr \, K_X}, \tag{2}$$

and where $Fr = V/\sqrt{gL}$ is the longitudinal hull Froude number. In order to account for the anisotropic geometry of a real ship's hull in a simple manner, we consider an elliptical pressure field of the form

$$P(X, Y) = F\left(X^2 + \frac{Y^2}{\mathcal{W}^2}\right), \tag{3}$$

where $\mathcal{W} = l/L$ is the aspect ratio of the ellipse of major diameter L and minor diameter l. Consistently with this choice, we let the elliptical change of variables

$$
\begin{aligned}
X &= \check{R} \cos \check{\varphi} & K_X &= \check{K} \, \cos \check{\theta} \\
Y &= \mathcal{W} \check{R} \sin \check{\varphi} & K_Y &= \mathcal{W}^{-1} \check{K} \sin \check{\theta} \, .
\end{aligned}
\tag{4}
$$

This leads to $Z(X, Y) = \check{Z}(\check{R}, \check{\varphi})$ where

$$\check{Z}(\check{R}, \check{\varphi}) = -\lim_{\tilde{\varepsilon} \to 0} \iint \check{K} \mathrm{d}\check{K} \mathrm{d}\check{\theta} \frac{\sqrt{\mathcal{W}^2 \cos^2 \check{\theta} + \sin^2 \check{\theta}} \, \check{\check{P}}(\check{K}) \, e^{-i\check{K}\check{R}\cos(\check{\theta} - \check{\varphi})}}{\sqrt{\mathcal{W}^2 \cos^2 \check{\theta} + \sin^2 \check{\theta}} - \mathcal{V}^2 \check{K} \cos^2 \check{\theta} + 2i\tilde{\varepsilon} \, \mathcal{V} \sqrt{\mathcal{W}} \cos \check{\theta}} , \tag{5}$$

and where $\mathcal{V} = Fr \sqrt{\mathcal{W}}$ and $\check{\check{P}}(\check{K}) = \mathcal{W}^{-1} \hat{P}(K_X, K_Y)$. The interest of the elliptical change of variables in Eq. (5) is that the Fourier transform of the pressure field is now a function of the single variable $\check{K}$. This, as we shall see later, implies that our previous derivation with an axisymmetric pressure field[11] is applicable to the case of an elliptical pressure field. Using the Sokhotski-Plemelj

formula (see, e.g., Ref. 20) to perform the integral over $\check{K}$ yields $\check{Z}(\check{R}, \check{\varphi}) = \check{Z}_0(\check{R}, \check{\varphi}) + \check{G}(\check{R}, \check{\varphi})$ where $\check{G}(\check{R}, \check{\varphi})$ is a rapidly decreasing function with the distance to the perturbation and where

$$\check{Z}_0(\check{R}, \check{\varphi}) = i\pi \int_{-\pi/2}^{\pi/2} d\check{\theta} \; \frac{(\mathcal{W}^2 \cos^2 \check{\theta} + \sin^2 \check{\theta}) \, \check{P}(\check{K}_0) \, e^{-i \check{K}_0 \check{R} \cos(\check{\theta} - \check{\varphi})}}{\mathcal{V}^4 \cos^4 \check{\theta}}, \tag{6}$$

where $\check{K}_0 = \sqrt{\mathcal{W}^2 \cos^2 \check{\theta} + \sin^2 \check{\theta}}/(\mathcal{V}^2 \cos^2 \check{\theta})$. The integral in Eq. (6) is of the form $\int d\check{\theta} \, H(\check{\theta}) \, e^{i \, \phi(\check{\theta})}$ and may be approximated through the method of the stationary phase. For $\check{R}/\mathcal{V}^2 > 1$, the integrand oscillates rapidly and there are two stationary points $\check{\theta}_1$ and $\check{\theta}_2$ given by $\phi'(\check{\theta}) = 0$. One can then write $\check{Z}_0(\check{R}, \check{\varphi}) \simeq i\pi(\check{Z}_{01}(\check{R}, \check{\varphi}) + \check{Z}_{02}(\check{R}, \check{\varphi}))$, where $\check{Z}_{01}$ corresponds to the transverse waves and $\check{Z}_{02}$ corresponds to the diverging waves. For large Froude numbers, the transverse waves vanish compared to the diverging waves,[11] so that within this limit we shall only consider the latter

$$\check{Z}_{02}(\check{R}, \check{\varphi}) = \check{Q}(\check{R}, \check{\varphi}) \, e^{i\left(\phi(\check{R}, \check{\theta}_2(\check{\varphi}), \check{\varphi}) + \frac{\pi}{4}\right)}, \tag{7}$$

where $\check{Q}(\check{R}, \check{\varphi})$ is the envelope of the wave signal

$$\check{Q}(\check{R}, \check{\varphi}) = \sqrt{\frac{2\pi}{\left|\partial_{\check{\theta}}^2 \phi(\check{R}, \check{\theta}_2(\check{\varphi}), \check{\varphi})\right|}} \; H(\check{\theta}_2). \tag{8}$$

For small elliptical angles $\check{\varphi}$, the stationary point $\check{\theta}_2$ reads $\check{\theta}_2(\check{\varphi}) = \pi/2 + 2\check{\varphi}$, and the envelope $\check{Q}(\check{R}, \check{\varphi})$ of the waves eventually becomes in the small $\check{\varphi}$ approximation

$$\check{Q}(\check{R}, \check{\varphi}) \simeq \frac{1}{4}\sqrt{\frac{\pi}{\check{R}}} \frac{1}{\mathcal{V}^3 \check{\varphi}^{5/2}} \check{P}\left(\frac{1}{4 \, \mathcal{V}^2 \check{\varphi}^2}\right). \tag{9}$$

It is worth mentioning here that we recover a very similar expression to that of the isotropic case,[11] where the hull Froude number Fr has been replaced by $\mathcal{V}$, and φ by $\check{\varphi}$. Let us now change the variables back to real polar coordinates (R, φ),

$$R = \check{R} \left(\cos^2 \check{\varphi} + \mathcal{W}^2 \sin^2 \check{\varphi}\right)^{1/2}, \tag{10a}$$

$$\varphi = \arctan(\mathcal{W} \tan \check{\varphi}). \tag{10b}$$

For small angles, Eqs. (10a) and (10b) become

$$R \simeq \check{R}, \tag{11a}$$

$$\varphi \simeq \mathcal{W} \check{\varphi}. \tag{11b}$$

Combining Eqs. (9) and (11a)–(11b) and defining the rescaled envelope in real polar coordinates $Q(R, \varphi) = \sqrt{\mathcal{W}} \, \check{Q}(\check{R}, \check{\varphi})$, one gets

$$Q(R, \varphi) \simeq \frac{1}{4}\sqrt{\frac{\pi}{R}} \frac{\mathcal{U}^3}{\varphi^{5/2}} \check{P}\left(\frac{\mathcal{U}^2}{4\varphi^2}\right), \tag{12}$$

where $\mathcal{U} = \mathcal{W} \mathcal{V}^{-1} = \sqrt{\mathcal{W}} \, Fr^{-1}$. This shows that the rescaled envelope $Q(R, \varphi)$ depends on the aspect ratio $\mathcal{W}$ and the rescaled Froude number $\mathcal{V}$ only through the single variable $\sqrt{\mathcal{W}} \, Fr^{-1}$. In other terms, for large Froude numbers and small angles, profiles resulting from moving disturbances with the same $\sqrt{\mathcal{W}} \, Fr^{-1}$ coincide when multiplied by $\sqrt{\mathcal{W}}$ (see Fig. 1). In particular, the angle φ_{max} corresponding to the maximum amplitude of the waves reads

$$\varphi_{max} \sim \frac{\sqrt{\mathcal{W}}}{Fr}. \tag{13}$$

This may explain why objects with very low aspect ratio, such as rowing boats, usually display a small maximum amplitude angle even though their longitudinal hull Froude number is not very high as they are propelled by man power.
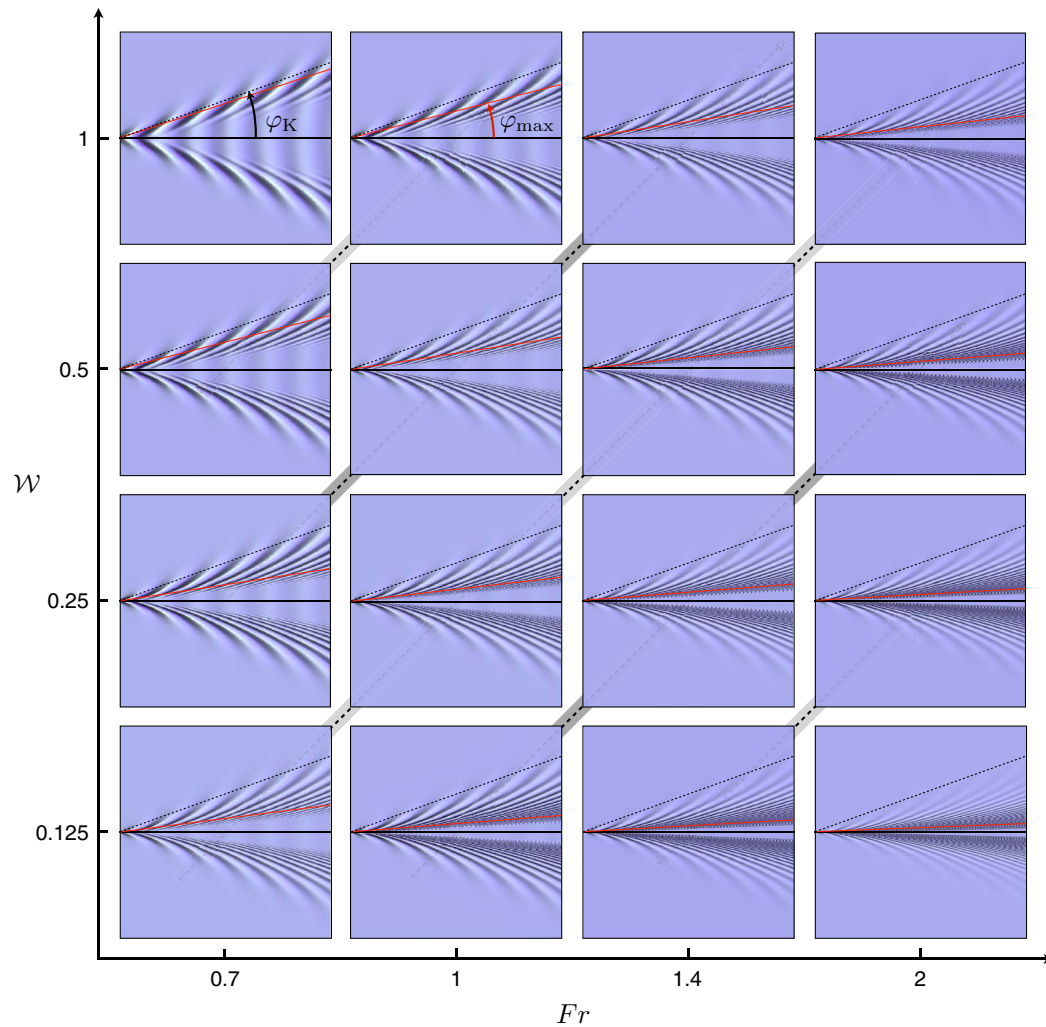
FIG. 1. Relief plots of the rescaled surface displacement produced by a moving elliptical Gaussian pressure field (see Eq. (14)) computed using Eq. (6). Here, rescaled means multiplied by $\sqrt{\mathcal{W}}$. Each relief plot corresponds to given values of the longitudinal hull Froude number Fr and aspect ratio $\mathcal{W}$ and is plotted as a function of $\tilde{X} = X/\Lambda$ and $\tilde{Y} = Y/\Lambda$ where $\Lambda = 2\pi Fr^2$ is the dimensionless wavelength. The parameters Fr and $\mathcal{W}$ are varied, respectively, along the horizontal axis and the vertical axis on a logarithmic scale. In all graphs, the angle $\varphi_{\max}$ indicating the maximum amplitude of the waves is signified with a solid line (red) and the Kelvin angle $\varphi_{K} = 19, 47°$ with a black dashed line. On each diagonal, signified by a grey stripe, the value of the ratio $\mathcal{U} = \sqrt{\mathcal{W}} \, Fr^{-1}$ is kept constant. The first row ($\mathcal{W} = 1$) corresponds to the isotropic case.

To illustrate these analytical results, we then perform a numerical evaluation of the integral in Eq. (6) with an elliptical Gaussian pressure field whose dimensionless Fourier transform reads

$$\hat{P}(K, \theta) = \frac{f_0}{\rho g L^3} \exp\left[-\frac{K^2}{4\pi^2}(\cos^2\theta + \mathcal{W}^2 \sin^2\theta) \right], \tag{14}$$

where f_0 is the total integrated pressure force. The resulting rescaled surface profiles are displayed in Fig. 1. Here, rescaled means multiplied by $\sqrt{\mathcal{W}}$. Each relief plot corresponds to given values of Fr and $\mathcal{W}$ and is plotted as a function of $\tilde{X} = X/\Lambda$ and $\tilde{Y} = Y/\Lambda$ where $\Lambda = 2\pi Fr^2$ is the dimensionless wavelength. The parameters Fr and $\mathcal{W}$ are varied, respectively, along the horizontal axis and the vertical axis on a logarithmic scale. In all graphs, the angle $\varphi_{\max}$ indicating the maximum amplitude of the waves is signified with a solid line (red) and the Kelvin angle φ_{K} with a black dashed line. On each diagonal, signified by a grey stripe, the value of the ratio $\mathcal{U} = \sqrt{\mathcal{W}} \, Fr^{-1}$ is kept constant. The first row ($\mathcal{W} = 1$) corresponds to the isotropic case. First, one can see that for any set

of parameters $(Fr, \mathcal{W})$ the angle delimiting the region outside which the surface remains essentially flat is constant and equal to the Kelvin angle φ_K. Second, on a given diagonal $(\sqrt{\mathcal{W}} \, Fr^{-1} = cst)$, all the profiles seem identical to the naked eye, therefore comforting the analytical results found in this section. Finally, looking closely, one can note that the agreement between different profiles on the same diagonal becomes all the more true as we go towards higher values of Fr, as predicted by the analytical study.

III. WAVE RESISTANCE

The waves generated by the moving disturbance continually remove energy to infinity. This translates into a drag force R experienced by the disturbance, often referred to as the wave drag or the wave resistance. We here investigate the wave resistance experienced by the disturbance, using the method proposed by Havelock,[17,19] according to whom the wave resistance is the total resolved pressure in the direction of motion

$$R = -\iint \mathrm{d}x \, \mathrm{d}y \, p(x, y) \, \partial_x \zeta(x, y). \tag{15}$$

Inserting Eq. (1) into Eq. (15) yields[21]

$$R = \lim_{\varepsilon \to 0} \iint \frac{\mathrm{d}k_x \, \mathrm{d}k_y}{4\pi^2 \rho} \, \frac{i k_x k \left| \hat{p}(k_x, k_y) \right|^2}{\omega^2(k) - V^2 k_x^2 + 2i\varepsilon V k_x}. \tag{16}$$

Changing to dimensionless variables consistently with Sec. II, switching to polar coordinates, and inserting the dimensionless elliptical Gaussian pressure field defined in Eq. (14) into Eq. (16) leads to

$$R = \lim_{\tilde{\varepsilon} \to 0} \left(\frac{f_0^2}{4\pi^2 \rho g L^3} \iint \mathrm{d}K \mathrm{d}\theta \, \frac{i K^2 \cos\theta \exp\left(-\frac{K^2}{2\pi^2}\left(\cos^2\theta + \mathcal{W}^2 \sin^2\theta\right)\right)}{1 - Fr^2 K \cos^2\theta + 2i\tilde{\varepsilon} Fr \cos\theta} \right). \tag{17}$$

Performing the integral over K in Eq. (17) yields

$$R = \frac{f_0^2}{2\pi \rho g L^3} \, f(\mathcal{V}, \mathcal{W}), \tag{18}$$

where

$$f(\mathcal{V}, \mathcal{W}) = \frac{\mathcal{W}^3}{\mathcal{V}^6} \int_0^{\pi/2} \frac{\mathrm{d}\theta}{\cos^5\theta} \exp\left(-\frac{\mathcal{W}^2(1 + \mathcal{W}^2 \tan^2\theta)}{2\pi^2 \mathcal{V}^4 \cos^2\theta}\right). \tag{19}$$

Equations (18) and (19) are central as they give the wave resistance of an elliptical Gaussian pressure field as a function of the dimensionless parameters $\mathcal{V}$ and $\mathcal{W}$. In order to seek for a limit form of the wave resistance at low aspect ratios, and guided by the fact that the integrand is dominant in the vicinity of $\pi/2$, this being all the more true for large values of $\mathcal{V}$ and small values of $\mathcal{W}$, we develop the integrand in the vicinity of $\pi/2$ at the lowest relevant order in θ and let the change of variables $\alpha = \pi/2 - \theta$. This yields

$$f(\mathcal{V}, \mathcal{W}) \simeq \frac{\mathcal{W}^3}{\mathcal{V}^6} \int_0^{\pi/2} \frac{\mathrm{d}\alpha}{\alpha^5} \exp\left(-\frac{\mathcal{W}^2}{2\pi^2 \mathcal{V}^4}\left(\frac{\mathcal{W}^2}{\alpha^4} + \frac{1}{\alpha^2}\right)\right). \tag{20}$$

Furthermore, aiming for a Gaussian like analytical integral, we let the change of variables $m = 1/\alpha^2$. This leads to

$$f(\mathcal{V}, \mathcal{W}) \simeq \frac{\mathcal{W}^3}{2\mathcal{V}^6} \int_{4/\pi^2}^{\infty} \mathrm{d}m \, m \, \exp\left(-\frac{\mathcal{W}^2}{2\pi^2 \mathcal{V}^4}\left(\mathcal{W}^2 m^2 + m\right)\right)$$

$$\simeq \frac{e^{-\frac{2\mathcal{W}^2(\pi^2 + 4\mathcal{W}^2)}{\pi^6 \mathcal{V}^4}}}{8\mathcal{V}^4 \mathcal{W}} \left[4\pi^2 \mathcal{V}^2 - \pi^{3/2}\sqrt{2} \, e^{\frac{(\pi^2 + 8\mathcal{W}^2)^2}{8\pi^6 \mathcal{V}^4}} \, \mathrm{erfc}\left(\frac{\pi^2 + 8\mathcal{W}^2}{2\pi^3 \sqrt{2}\mathcal{V}^2}\right)\right], \tag{21}$$
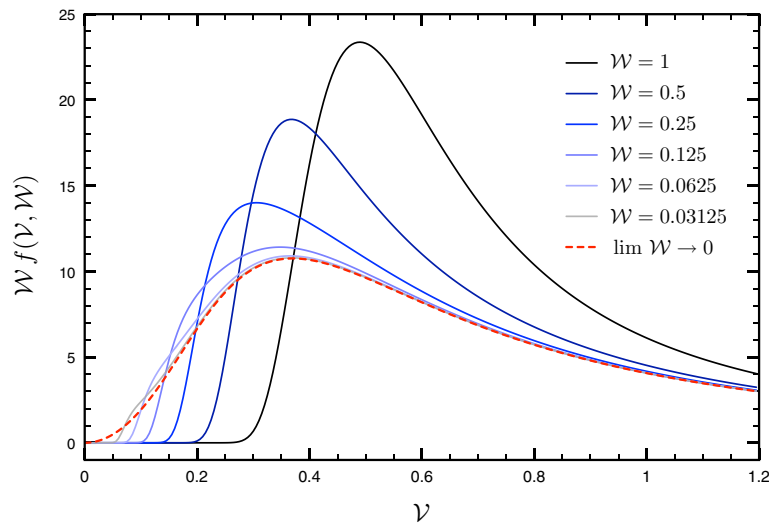
FIG. 2. Plot of $\mathcal{W} f(\mathcal{V}, \mathcal{W})$ as given by Eq. (21) as a function of the dimensionless parameter $\mathcal{V} = Fr \sqrt{\mathcal{W}}$, where $Fr = V/\sqrt{gL}$ is the longitudinal hull Froude number, for different values of the aspect ratio $\mathcal{W}$. The dashed curve (red) corresponds to the limit regime $\mathcal{W} \to 0$ as given analytically by Eq. (22).

where erfc $= 1 -$ erf is the complementary error function.[22] In the limit of small aspect ratios $\mathcal{W}$, $f(\mathcal{V}, \mathcal{W})$ scales as $1/\mathcal{W}$ and

$$\lim_{\mathcal{W} \to 0} \mathcal{W} f(\mathcal{V}, \mathcal{W}) = \frac{\pi^2}{2\mathcal{V}^2} - \frac{\pi^{3/2}\sqrt{2}}{8\mathcal{V}^4} \exp\left(\frac{1}{8\pi^2\mathcal{V}^4}\right) \text{erfc}\left(\frac{1}{2\pi\sqrt{2}\mathcal{V}^2}\right). \tag{22}$$

Equation (22) provides an analytical limit of the wave resistance at very low aspect ratios $\mathcal{W}$. The fact that this limit is independent of $\mathcal{W}$ shows that $\mathcal{V}$ is the relevant variable to describe the problem of anisotropic moving objects. Figure 2 displays $\mathcal{W} f(\mathcal{V}, \mathcal{W})$ as given by Eq. (21) as a function of $\mathcal{V}$ for different values of the aspect ratio $\mathcal{W}$. The dashed curve (red) corresponds to the limit regime $\mathcal{W} \to 0$ as given analytically by Eq. (22). As one can see, the curves converge to the limit regime $\mathcal{W} \to 0$ as the aspect ratio is decreased, the convergence being faster at large $\mathcal{V}$. In the limit of small aspect ratios, the position of the maximum of wave resistance $\mathcal{V}_{\max}$ is obtained numerically by solving $\frac{d}{d\mathcal{V}} (\lim_{\mathcal{W} \to 0} \mathcal{W} f(\mathcal{V}, \mathcal{W})) = 0$; one gets $\mathcal{V}_{\max} \simeq 0.3702$. Recalling that $\mathcal{V} = Fr \sqrt{\mathcal{W}}$, one has the scaling of the position of the maximum of wave resistance in terms of Froude number

$$Fr_{\max} \sim \frac{1}{\sqrt{\mathcal{W}}} , \tag{23}$$

or identically in terms of real speed

$$V_{\max} \sim \sqrt{\frac{gL}{\mathcal{W}}} = \sqrt{gL} \sqrt{\frac{L}{l}} . \tag{24}$$

It is known that for cylindrical objects of size L, the position of the maximum of wave resistance scales as[23] $\sqrt{gL}$. Equation (24) shows that in our case, the scaling is that of the cylindrical object multiplied by the square root of the inverse aspect ratio. Note that, in order to discuss the amplitude of wave resistance rather than the position of its maximum, one must prescribe how the total integrated force f_0 behaves with the dimensions of the distribution. For example, one could have f_0 proportional to the area $Ll = L^2\mathcal{W}$, and given that the wave resistance behaves as f_0^2, the relevant quantity to plot would be $\mathcal{W}^2 f(\mathcal{V}, \mathcal{W})$.

Recently, Noblesse et al.[10] analyzed the observations of Rabaud and Moisy[9] in terms of interference between the dominant bow and stern waves created by the ship, assuming a pressure field of dipolar nature. Note that their analysis leads to additional interference peaks in the wave resistance at small Froude numbers, in accordance with a number of observations.

IV. CONCLUSION

In this study, we performed a theoretical analysis of the wake pattern and the wave resistance of an anisotropic moving disturbance. In order to account for anisotropy in a simple manner, we modelled the disturbance by an elliptical pressure distribution. In Sec. II, we derived the expression of the surface displacement and analyzed it as a function of two relevant dimensionless parameters. We showed that the angle delimiting the wake region remains constant and equal to the Kelvin angle $\varphi_K = 19.47°$; and that, at large Froude numbers, the angle corresponding to the maximum amplitude of the waves scales as $\sqrt{\mathcal{W}}/Fr$ where $\mathcal{W}$ is the aspect ratio of the elliptical disturbance and Fr is the longitudinal hull Froude number. This notably extends the results of our previous study[11] that focused on isotropic moving objects. Note that very recently similar results have been obtained independently by Moisy and Rabaud.[24] Another study[25] by the same authors where capillary effects are taken into account may also be of interest to the readers. In Sec. III, we derived the expression of the wave resistance for an elliptical Gaussian pressure field and analyzed it as a function of the same relevant dimensionless parameters. We obtained a limit analytical expression for the case of very small aspect ratios, and showed that the position of the maximum of wave resistance in terms of real speed scales as that of a cylindrical object multiplied by the square root of the inverse aspect ratio. We believe this study is of interest as it reveals the main physical features of waves created by anisotropic moving objects, closer to the real geometry of ships than axisymmetric objects.

[1] L. Kelvin, "On the waves produced by a single impulse in water of any depth," Proc. R. Soc. London, Ser. A **42**, 80–83 (1887).
[2] J. Lighthill, *Waves in Fluids* (Cambridge University Press, Cambridge, 1978).
[3] A. Barnell and F. Noblesse, "Far-field features of the kelvin wake," in *Proceedings of the 18th Symposium on Naval Hydrodynamics, Washington DC* (David W. Taylor Naval Ship Research and Development Center, 1986), pp. 465–476.
[4] H. Lamb, *Hydrodynamics*, 6th ed. (Cambridge University Press, Cambridge, 1993).
[5] R. S. Johnson, *A Modern Introduction to the Mathematical Theory of Water Waves* (Cambridge University Press, 1997).
[6] F. Dias and C. Kharif, "Nonlinear gravity and capillary-gravity waves," Annu. Rev. Fluid Mech. **31**, 301–346 (1999).
[7] S. Å. Ellingsen and I. Brevik, "How linear surface waves are affected by a current with constant vorticity," Europ. J. Phys. **35**, 025005 (2014).
[8] S. Å. Ellingsen, "Ship waves in the presence of uniform vorticity," J. Fluid Mech. **742**, R2 (2014).
[9] M. Rabaud and F. Moisy, "Ship wakes: Kelvin or mach angle?" Phys. Rev. Lett **110**, 214503 (2013).
[10] F. Noblesse, J. He, Y. Zhu, L. Hong, C. Zhang, R. Zhu, and C. Yang, "Why can ship wakes appear narrower than kelvins angle?" Eur. J. Mech. B **46**, 164–171 (2014).
[11] A. Darmon, M. Benzaquen, and E. Raphaël, "Kelvin wake pattern at large froude numbers," J. Fluid Mech. **738**, R3 (2014).
[12] F. Dias, "Ship waves and kelvin," J. Fluid Mech, Focus Fluids **746**, 1–4 (2014).
[13] E. M. Casling, "Planing of a low-aspect-ratio flat ship at infinite froude number," J. Eng. Math. **12**, 43–57 (1978).
[14] B. M. Taravella and W. S. Vorus, "A general solution to low-aspect-ratio flat-ship theory," J. Eng. Math. **71**, 171–184 (2011).
[15] D. Peri, M. Rossetti, and E. F. Campana, "Design optimization of ship hulls via cfd techniques," J. Ship Res. **45**, 140–149 (2001).
[16] O. Darrigol, *Words of Flow: A History of Hydrodynamics from the Bernoullis to Prandtl* (Oxford University, New York, 2005).
[17] T. H. Havelock, "The propagation of groups of waves in dispersive media, with application to waves on water produced by a traveling disturbance," Proc. R. Soc. A **81**, 398 (1908).
[18] J. V. Wehausen, "The wave resistance of ships," Adv. Appl. Mech. **13**, 93–245 (1973).
[19] T. H. Havelock, "Periodic irrotational waves of finite height," Proc. R. Soc. A **95**, 38–51 (1918).
[20] W. Appel, *Mathematics for Physics and Physicists* (Princeton University Press, 2007).
[21] E. Raphaël and P.-G. de Gennes, "Capillary gravity waves caused by a moving disturbance: Wave resistance," Phys. Rev. E **53**, 3448 (1996).
[22] M. Abramowitz and I. A. Stegun, *Handbook of Mathematical Functions: With Formulas, Graphs, and Mathematical Tables* (Courier Dover Publications, 2012).
[23] J. J. Stoker, *Water Waves: The Mathematical Theory with Applications* (Wiley-Blackwell, 1992).
[24] F. Moisy and M. Rabaud, "Scaling of far-field wake angle of non-axisymmetric pressure disturbance," Phys. Rev. E **89**, 063004 (2014).
[25] F. Moisy and M. Rabaud, "Mach-like capillary-gravity wakes," Phys. Rev. E **90**, 023009 (2014).